TITLE

Florigen and antiflorigen gene expression correlates with reproductive state in a marine angiosperm, *Zostera marina*

AUTHORS

Christine T. Nolan[1], Ian Campbell[1], Anna Farrell-Sherman[1,2], Bryan A. Briones Ortiz[3], Kerry A. Naish[3], Verónica Di Stilio[1], James E. Kaldy[4], Cinde Donoghue[5,6], Jennifer L. Ruesink[1], Takato Imaizumi[1]

[1]Department of Biology, University of Washington, Seattle, WA USA 98195
[2]Vaccine and Infectious Disease Division, Fred Hutch Cancer Center, Seattle, WA USA 98109
[3]School of Aquatic and Fishery Sciences, University of Washington, Seattle, WA USA 98195
[4]Pacific Ecological Systems Division, US EPA, Newport, OR USA 97365
[5]Washington Department of Natural Resources, Olympia, WA USA 98504
[6]Washington Department of Ecology, Lacey, WA USA 98503

Corresponding author: Takato Imaizumi, takato@uw.edu

Word Count Total: 7,090
- Introduction: 1,198
- Materials & Methods: 2,071
- Results: 1,985
- Discussion: 1,596
- Conclusion: 240

Figures in main text (published in color): 5
Figures in supplemental information (published in color): 8
Tables in supplemental information: 12

SUMMARY

- Florigen and antiflorigen genes within the phosphatidylethanolamine-binding protein (PEBP) family regulate flowering in angiosperms. In eelgrass (*Zostera marina*), a marine foundation species threatened by climate change, flowering and seed production are crucial for population resilience. Yet, the molecular mechanism underpinning flowering remains unknown.
- Using phylogenetic analysis and functional assays in *Arabidopsis*, we identified thirteen *PEBP* genes in *Z. marina* (*ZmaPEBP*) and showed that four genes altered flowering phenotypes when overexpressed. We used quantitative RT-PCR on *Z. marina* shoots from perennial and annual populations in Willapa Bay, USA to assess expression of these four genes in different tissue and expression changes throughout the growth season.
- We demonstrated that *ZmaFT2* and *ZmaFT4* promote flowering, and *ZmaFT9* and *ZmaTFL1a* repress flowering in *Arabidopsis*. Across five natural sites exhibiting different degrees of population genetic structure, *ZmaFT2* and *ZmaFT4* were expressed in leaves of vegetative and reproductive shoots and in stems and rhizomes of reproductive shoots. *ZmaFT9* was distinctively expressed in leaves of vegetative and juvenile shoots, while *ZmaTFL1a* levels increased after flowering shoots emerged.
- Our results suggest that *ZmaFT2* and *ZmaFT4* may promote flowering, while *ZmaFT9* may inhibit a floral transition in eelgrass. We speculate that *ZmaTFL1a* may be involved in flowering shoot architecture.

KEYWORDS

antiflorigen, florigen, flowering, foundation species, phosphatidylethanolamine-binding proteins (PEBP), seed production, *Zostera marina* (eelgrass)

INTRODUCTION

In angiosperms, flowering is induced by florigen (flowering-inducing substrate) genes, with *FLOWERING LOCUS T* (*FT*) as the main inducer of flowering processes. *FT* is a member of a larger family of genes that encode phosphatidylethanolamine-binding proteins (PEBP),

which includes other genes relevant to flowering, all of which are highly conserved across flowering plants (Pin & Nilsson, 2012; Wickland & Hanzawa, 2015). In *Arabidopsis thaliana*, there are six *FT*-like genes implicated in flowering and reproductive processes. *FT* and *TWIN SISTER OF FT* (*TSF*) generate small proteins that move through the plant to the shoot apical meristem, and both activate flowering (florigen); as such, they have redundant effects (Kardailsky *et al.*, 1999; Yamaguchi *et al.*, 2005; Corbesier *et al.*, 2007). *TERMINAL FLOWER 1* (*TFL1*), *CENTRORADIALIS* (*ATC*), and *BROTHER OF FT AND TFL1* (*BFT*) all inhibit the onset of flowering (Kobayashi *et al.*, 1999; Mimida *et al.*, 2001; Yoo *et al.*, 2010). *MOTHER OF FT AND TFL1* (*MFT*), while capable of activating flowering processes, also plays a role in seed germination (Yoo *et al.*, 2004; Xi *et al.*, 2010). In *Arabidopsis*, *PEBP* genes involved with the photoperiodic flowering pathway show tissue-specific expression patterns. *FT* is primarily expressed in leaf phloem companion cells, generating a protein that acts as a long distance signal transported through the phloem (Takada & Goto, 2003; Corbesier *et al.*, 2007). *TFL1* expression occurs in meristem tissue in shoots in *Arabidopsis* and both *FT* and *TFL1* play a role in shoot indeterminacy and maintenance of vegetative state (Bradley *et al.*, 1997; Ratcliffe *et al.*, 1999; Baumann *et al.*, 2015; Liu *et al.*, 2023b). The *PEBP* gene family has undergone expansion in monocot lineages, specifically within the *FT* clade, with species like *Oryza sativa* and *Brachypodium distachyon* having 19 and 18 members of their *PEBP* gene families (13 and 12 within *FT* clades), respectively (Itoh *et al.*, 2010; Wu *et al.*, 2013; Bennett & Dixon, 2021; Liu *et al.*, 2023a). *PEBP* genes have multifaceted roles in plant growth and development in other plant species; *FT* and *TFL1* are both known to affect branching and shoot architecture in flowering plants including *Arabidopsis* and tomato (Niwa *et al.*, 2013; Lifschitz *et al.*, 2014; Weng *et al.*, 2016). *FT* homologs have also been shown to promote tuber and stolon formation in potatoes and strawberries, respectively (Navarro *et al.*, 2011; Gaston *et al.*, 2021). *FT* expression is mainly controlled by photoperiod (daylength) and temperature, among other environmental conditions, which in turn regulates flowering time (Blázquez *et al.*, 2003; Balasubramanian *et al.*, 2006; Lee *et al.*, 2007; de Montaigu *et al.*, 2010; Song *et al.*, 2013; Kinmonth-Schultz *et al.*, 2016; Susila *et al.*, 2018; Takagi *et al.*, 2023).

Because flowering directly impacts seed production and fruit yield in plant reproduction, *FT* function and the floral pathway have been extensively studied in a wide breadth of terrestrial plant species (Wickland & Hanzawa, 2015), including dicots such as *Beta vulgaris* (Pin *et al.*,

2010) and *Chrysanthemum setiscupe* (Oda *et al.*, 2012), and also monocot species such as *Allium cepa* (Lee *et al.*, 2013) and *Oryza sativa* (Kojima *et al.*, 2002). Characterization of *FT* function in aquatic species has only been recently explored in fresh-water species (Yoshida *et al.*, 2021), and has not yet been investigated in marine angiosperm species. Eelgrass (*Zostera marina*) is a seagrass native to both the Atlantic and Pacific Northern Hemisphere, one of about 60 species of marine angiosperms and a member of the early-diverging monocot order *Alismatales*. Despite its small genome of 202.3 Mb (Olsen *et al.*, 2016), eelgrass is predicted to have at least thirteen *PEBP* genes (Liu *et al.*, 2023a) in line with the observed expansion in other monocot lineages.

Seagrasses are foundation species and broadly are key components of marine coastal ecosystems essential for nutrient cycling, sediment stabilization, and habitats for fish and invertebrates (Orth *et al.*, 2006; Hays *et al.*, 2021). However, seagrasses are highly sensitive to natural and anthropogenic pressures such as eutrophication, shading, and direct bed disturbances, and experience higher mortality rates with higher water temperatures (Orth *et al.*, 2006; Nejrup & Pedersen, 2008). Flowering and seed production play a key role in contributing to persistence and increasing genetic diversity within local *Z. marina* populations, and restoration efforts centered around seeds appear promising (Marion & Orth, 2010; Kendrick *et al.*, 2012; Orth *et al.*, 2012, 2020; van Katwijk *et al.*, 2016; Cronau *et al.*, 2023). Annual and perennial forms of eelgrass exist and are largely regarded as distinct ecotypes. In annual ecotypes, seeds germinate and shoots flower within one season (Robertson & Mann, 1984; Ruesink *et al.*, 2022), whereas in perennial ecotypes, the predominant form, shoots persist for multiple seasons and populations as a whole produce far fewer flowering shoots with large variation in flowering frequency (Ruesink *et al.*, 2022). Yet eelgrass shows large phenotypic variation, especially in flowering timing and frequency across spatial scales and seasons (Thom *et al.*, 2003; Yang *et al.*, 2013; Qin *et al.*, 2020; Ruesink *et al.*, 2022). Determining the causes for this variation is central to understanding the ecology, evolution, and restoration of the species.

In perennial populations of *Z. marina* in Willapa Bay, less than 25% of shoots typically flower each year (Thom *et al.*, 2003; Ruesink *et al.*, 2022), and it is not currently possible to predict how many and which shoots will flower. Therefore, studying the genetic and molecular mechanism of flowering onset in perennial populations proves very difficult. In the annual ecotype, all shoots flower in the same year as germination, such that populations dominated by annuals can exceed 70% flowering frequency (Phillips *et al.*, 1983; Keddy, 1987; Ruesink *et al.*,

2022). Characterizing the mechanism underpinning sexual reproduction and its relationship to environmental stimuli in *Z. marina* is a key knowledge gap that if addressed, would improve our understanding of how seed production is affected by local environmental factors. Further, identifying genetic markers of flowering would provide a method for predicting seed potential within a population. Such advances could ultimately allow for more strategic and efficient seed-based restoration efforts of eelgrass, through improved donor site selection and in the scaling-up of seed collection and planting efforts (Harwell & Rhode, 2007; van Katwijk *et al.*, 2016; Orth *et al.*, 2020). However, the relevant genes and mechanism by which *Z. marina* flowering onset is cued and regulated across populations remains completely unknown.

Here, we explored the mechanism of flowering in *Z. marina* and investigated the function of *FT/TFL1* homologs. We confirmed thirteen eelgrass florigen homologs (*ZmaPEBP*) and demonstrated that four are likely functionally relevant to the flowering pathway, both as activators and repressors. To elucidate *ZmaPEBP* gene function, we performed a heterologous functional assay in *Arabidopsis thaliana*. Overexpression of four *ZmaPEBP* genes, *ZmaFT2*, *ZmaFT4*, *ZmaFT9*, and *ZmaTFL1a,* resulted in either precocious or delayed flowering. We characterized expression patterns of these four genes in *Z. marina* shoots across three perennial sites and three annual sites to rule out patterns that are site- or life history- specific. Quantification of expression of these four genes across different tissue types and developmental stages suggests that *ZmaFT9* may play a role in the repression of flowering and *ZmaFT2* and *ZmaFT4* may contribute to flowering onset, while *ZmaTFL1a* likely functions in flowering shoot architecture.

MATERIALS & METHODS

Phylogenetic analysis and identifying *ZmaPEBP* genes

To identify *PEBP* family members and possible *FT* homologs in *Z. marina*, we performed a BLAST search (Altschul *et al.*, 1990) using the *Arabidopsis* FT (AT1G65480) amino acid sequence against the *Z. marina* genome (Olsen *et al.*, 2016). DNA sequences of *PEBP* family genes were obtained from the literature (Table S1), or from the genomes of the order *Alismatales* via a BLAST search with the *A. thaliana FT* and *Z. marina FT-like* sequence as queries. Sequences included previously described *PEBP* family genes from *A. thaliana*, *Oryza*

sativa, Aquilegia coerulea, Chrysanthemum seticuspe, and *Brachypodium distrachyon* along with all recovered full-length *Alismatales* family *PEBP* genes, including *Z. marina*. To gain insight into the evolution and expansion of the *PEBP* gene family within other *Zostera* species, we included *Zostera muelleri* (Lee *et al.*, 2016). *Z. muelleri PEBP* genes were identified via local BLAST search in its genome using *A. thaliana FT* sequences as query.

To create a phylogenetic tree, all full-length *Alismatales* sequences were aligned with previously described *PEBP* family sequences from *A. thaliana*, *O. sativa, A. coerulea, C. seticuspe,* and *B. distrachyon* by Multiple Sequence Comparison by Log-Expectation (MUSCLE) on the EMBL-EBI portal (Madeira *et al.*, 2024). The alignment was fine-tuned by hand in Mesquite v 3.70 with the Multiple Sequence Alignment module (Maddison & Maddison, 2023). We used IQ-TREE (Nguyen *et al.*, 2014) to build a maximum-likelihood phylogenetic tree with 1000 bootstraps using ModelFinder (Kalyaanamoorthy *et al.*, 2017) to predict the best substitution matrix and UFBoot (Hoang *et al.*, 2018) to compute ultra-fast bootstrap values. Mesquite Version 3.70 was used to build the consensus tree out of 400 base trees including sequences from *Z. marina, Z. muelleri, A. thaliana, B. distachyon, A. coerulea, Lemna aequinoctialis, Symplocarpus renifolius, Spirodela polyrhiza, C. seticuspe, O. sativa*, and *Allium cepa*.

Key amino acid residues that have been important in canonical FT and TFL1 structure and function (Hanzawa *et al.*, 2005; Ho & Weigel, 2014) were analyzed using a multiple sequence alignment (MAFFT) (Katoh *et al.*, 2002) of amino acid sequences of *Z. marina*, *Arabidopsis* FT and TFL1 along with the rice *Oryza sativa* FT homolog Hd3a to have a monocot FT sequence as comparison.

Generating transgenic *ZmaPEBP* overexpression lines in *Arabidopsis* and quantifying flowering time

We used transgenic heterologous assays in *A. thaliana* to assess effect of *ZmaPEBP* genes on flowering and gain insights into overall function. All experiments in *A. thaliana* were performed in the wild-type Col-0 accession. To generate *35S:ZmaPEBP* transgenic lines, the coding sequences for each *ZmaPEBP* gene from the *Z. marina* reference genome (Olsen *et al.*, 2016) were synthesized (Twist Bioscience, South San Francisco CA) and amplified with locus-specific primers by PCR to remove any adapter sequences (Table S2, S3). Using Gateway

cloning, each gene was cloned into the pENTR D-TOPO vector (Invitrogen, Waltham MA), and after the insert sequences were verified by sequencing, they were transferred to the overexpression binary vector, pB7WG2 (Karimi *et al.*, 2002). We used *Agrobacterium tumefaciens* strain GV3101 harboring each vector construct to transform *Arabidopsis* wild-type (Col-0) plants with conventional floral-infiltration and selection methods (Weigel & Glazebrook, 2002). The *35S:GFP* line was generated in a similar manner to serve as a control.

To screen for altered flowering phenotypes in *35S:ZmaPEBP* transgenic lines, we used T_1 generation plants in the initial flowering time assay with all *35S:ZmaPEBP* and *35S:GFP* transgenic lines. In the T_1 flowering time assay, sterilized seeds were germinated on selection media [1xLinsmaier-Skoog (PhytoTech Labs, Lenexa KS) media, 2% sucrose (wt/vol), 100 mg/L ticarcillin, 16 µg/mL Basta] in long day (LD) condition (16 h light, 8 h dark, 100 µmol/m^2s, 22 °C). 14-day-old seedlings with resistance to selection medium were transferred to soil (Sunshine #4, Sun Gro Horticulture, Agawam MA) and moved into plant growth chambers with LD conditions (16 h light, 8 h dark, 100 µmol/m^2/s, 22 °C, 70% relative humidity). Flowering assays in the T_1 generation included at least 16 individuals per construct. We recorded rosette leaf number at time of flowering.

Candidate genes that yield altered flowering time phenotypes were assayed using homozygous T_3 plants with a single T-DNA insertion from *35S:ZmaPEBP* lines. In the T_3 flowering assays, sterilized seeds were sown directly into soil in plant growth chambers with LD conditions (16 h light, 8 h dark, 100 µmol/m^2/s, 22 °C, 70% relative humidity). We quantified flowering time in a similar manner in T_1 and T_3 lines. Flowering assays in the T_3 generation included at least 10 individuals per line.

Analyses of population genetic structure

In order to gain insight into the conserved nature of *ZmaPEBP* genes between populations and life history types, we described the genetic relatedness between meadows with annual and perennial ecotypes in close proximity to each other using sites in Willapa Bay, WA, USA. This well-studied estuary, located in the eastern Pacific Ocean, covers 240 km^2 at mean tide (Hickey & Banas, 2003) and contains 34 km^2 of eelgrass meadows occupying about a quarter of intertidal flats (Ruesink *et al.*, 2006). The bay contains *Z. marina* populations comprising both the perennial and annual ecotype, which show widespread phenotypic and

morphological variation, including temporal and population-specific variation in flowering frequency (Thom *et al.*, 2003; Ruesink *et al.*, 2022).

Population-level genetic structure was determined using reduced representation sequencing across five sites (RAD-seq; Figure 3 G, Table S4) (Ali *et al.*, 2016). We chose three perennial and two annual sites, where one site included both ecotypes in close proximity (<0.2 km separation) (Table S4). In April 2023, 50 shoots were collected from Bay Center and Long Island, with 1-2 m spacing between each individual in order to reduce the probability of collecting clones (Duffy *et al.*, 2022). The meristem region (3-5 cm) was saved from cleaned shoots and frozen in liquid nitrogen and stored at -80ºC (Briones Ortiz *et al.*, *In press*). Samples from Stackpole, Stackpole Annual, and Nahcotta Port Annual sites were collected in 2019 as described in Briones Ortiz et al (Briones Ortiz *et al.*, *In press*).

High-molecular-weight genomic DNA was extracted using DNeasy Plant Pro Kit (Qiagen, Hilden, Germany). Genomic libraries were constructed for restriction-site associated DNA sequencing (RAD-seq) (Ali *et al.*, 2016) with the restriction enzyme *Sbf1* and sequenced using the Illumina NovaSeq 6000 SP platform using 150 bp paired-end reads (University of Oregon, Genomics and Cell Characterization Core Facility, Eugene OR). Pooled-library reads were demultiplexed using the *process_radtags* program with *–best-rad* settings and trimmed to 137 bp in STACKS (Catchen *et al.*, 2013). The single-end reads were aligned to the published genome of *Z. marina* (Olsen *et al.*, 2016; Ma *et al.*, 2021), using BWA-MEM (Li, 2013), with minimum alignment and mapping Phred quality scores of 30.

Genotyping of polymorphic loci was conducted using the *ref_map* pipeline in STACKS (Rochette & Catchen, 2017). Subsequent filtering was performed using the R-package SNPFILTR (DeRaad, 2022)(steps described in Table S5). Identical multilocus genotypes (MLGs, >95% shared alleles between individuals), a result of clonal reproduction, were identified using PLINK (function –genome) (Chang *et al.*, 2015). Only one representative sample of each clonal genotype was retained for further processing. Samples in the Stackpole perennial and both annual sites were initially collected as seedlings resulting from sexual reproduction, and no clones were found.

Population structure was examined using measures of population genetic differentiation (F_{ST}) (Weir & Cockerham, 1984) using the R-package HIERFSTAT (Goudet, 2005; de Meeûs & Goudet, 2007). Population structure was also inferred using a test of population assignment of

individuals, implemented in STRUCTURE v2.1.1.5 (Pritchard *et al.*, 2000). The number of clusters (*K*) tested ranged from 1 to 10, and the most likely ancestral groups were evaluated using the mean log probability of the data, *L*(*K*) (Pritchard *et al.*, 2000) and the *ΔK* statistic (Evanno *et al.*, 2005). Genetic relationships among individual samples were visualized using a discriminant analysis of principal components (DAPC) plot, implemented in the R package ADEGENET (Jombart & Ahmed, 2011).

Collection of plant material, RNA extraction and quantitative RT-PCR

We used extracted RNA and quantitative RT-PCR (qPCR) to assess gene expression levels in both *Z. marina* and *A. thaliana* plant tissue. Gene expression was determined in three instances: *A. thaliana* T_1 and T_3 lines, and *Z. marina* in field collections. For gene expression analysis in T_1 lines, sterilized seeds were germinated on 1xLS 2% sucrose antibiotic selection media in LD conditions (16 h light, 8 h dark, 100 μmol/m^2s, 22 °C) to isolate successful transformed seedlings. At two weeks, seedlings were transferred to 1xLS media without sucrose and antibiotics. After one week, seedlings (21-day-old) were harvested at ZT16 (zeitgeber time). For gene expression analysis in T_3 lines, seeds were germinated on 1xLS media without sucrose in LD conditions (16 h light, 8 h dark, 100 μmol/m^2s, 22 °C). 14-day-old seedlings were collected at ZT16.

For gene expression analysis in *Z. marina* from the field, whole shoots and plant tissues (including rhizome and roots, vegetative mature leaves, inflorescence, and spathes) were collected from perennial population sites in Willapa Bay (Fig. 3, Table S4) in a three-consecutive-day period in mid-July (13-15 Jul 2022) between ZT3-5. We collected tissue from at least 15 adult plants at each site, with 1-2m spacing between each individual. Samples from two annual populations [ST-ANN and NP-ANN, (Ruesink *et al.*, 2022)] and one annual population from Yaquina Bay (YQ-ANN) were collected in a similar manner at two-week intervals between April and August 2023 between ZT3-5. All plant tissue collected was stored immediately in RNAlater stabilization solution (ThermoFisher, Waltham MA). Samples were moved to -80°C for long-term storage. Photoperiod data was obtained from the US Naval Astronomical Applications Department (Astronomical Applications Department, U. S. Naval Observatory, 2023). Temperature data was collected at the sediment surface using iButtons (Dallas Semiconductor, Dallas TX) in 2-hour increments at Willapa Bay Annual sites.

Total RNA was isolated from samples using RNeasy Plant Mini Kit (Qiagen, Hilden, Germany), including an on-column DNA digestion procedure. Complementary DNA (cDNA) was obtained with iScript cDNA synthesis kit (Bio-Rad, Hercules CA). We analyzed expression levels of the gene of interest with qPCR. The qPCR reaction was carried out on 2µL of 1/5-diluted cDNA using 2X SSoAdvance SYBR Super Mix (Bio-Rad, Hercules CA) with locus-specific primers (Table S2).

We used two reference genes to normalize expression in transgenic *Arabidopsis*, *ISOPENTENYL PYROPHOSPHATE / DIMETHYLALYLL PYROPHOSPHATE ISOMOERASE* (*IPP2*) and *SERINE/THREONINE PROTEIN PHOSPHOTASE 2A* (*PP2A*) (Song *et al.*, 2018). We used three previously described reference genes for expression analysis in *Z. marina* (Ransbotyn & Reusch, 2006), *CYCLOPHILIN 2* (*CYP2*), *EUKARYOTIC INITIATION FACTOR4A* (*ELF4A*), and *RIBOSOME STRUCTURAL PROTEIN L28* (*RPL28*). Samples with no detectable expression were treated as having a cycle threshold (C_T) value as C_T=40. A baseline threshold of relative fluorescence units (RFU) was set for consistency across primers to compare between plates, and resulting C_T values were analyzed using a delta C_T method. For the reference, the average C_T values of all reference genes were used for calculation.

Statistical analysis of *Z. marina* gene expression data

We performed statistical analyses on the *Z. marina* expression data to compare tissue-specific expression in flowering and vegetative life stages across three sites (Jul 2022), and to examine the time series of expression in annual eelgrass (Apr-Sep 2023). Expression of candidate genes (*ZmFT2*, *ZmFT4*, *ZmFT9*, and *ZmTFL1a*) were analyzed separately. In the first comparison, linear models (analysis of variance, ANOVA) were constructed with relative expression values (delta C_T) as response variable and with site, tissue, and life stage, as well as tissue x life stage interaction included as fixed factors. To be comparable between vegetative and flowering life stages, the included tissue types were rhizome, stem, and leaf middle (middle 10cm of leaf blade, Fig. 3).

In the second comparison, each of the eight collection timepoints was considered a separate level of a categorical factor, because different individuals were collected each time, and because gene expression could turn on or off abruptly. Using a linear mixed effects model framework, delta C_T was the response variable and fixed effects were time point and site.

Additionally, we tested for a site by time point interaction to that would account for different phenology between sites. Expression values required log-transformation to generate a Gaussian distribution in all analyses. Any significant factors or interactions were followed up by post-hoc tests to determine significant differences between groups based on Tukey HSD significance levels. Statistical models were built in R (R Core Team, 2024) using the package lme4 (Bates *et al.*, 2015), with post-hoc tests from emmeans (Searle *et al.*, 1980).

RESULTS

Phylogenetic analysis revealed thirteen *PEBP* genes in *Z. marina*

We identified thirteen *Z. marina* genes that fell within the *PEBP* gene family based on sequence homology. Phylogenetic analysis incorporating other *PEBP* genes representing different plant lineages revealed these thirteen genes belong to three clades; *FT/TSF* (ten genes, named *ZmaFT1-10*), *TFL1/BFT* (two genes, labeled *ZmaTFL1a* and *ZmaTFL1b*), and *MFT* (one gene, *ZmaMFT1*) (Fig. 1). Monocot lineages harbor an expansion in *FT* genes, and it has been shown that the initial *FT* duplication within monocots occurred in *Alismatales*, the basal monocot lineage that includes *Z. marina* and the *Zosteraceae* family (Bennett & Dixon, 2021). *Z. muelleri*, a sister species to *Z. marina*, has a similar gene duplication structure to *Z. marina*. Both *Z. marina* and *Z. muelleri* have multiple copies of *FT* beyond the initial duplication described in Bennett & Dixon (Bennett & Dixon, 2021) and have copies present in three *FT* subclades described in Liu et al. (Liu *et al.*, 2023a).

PEBP genes that activate flowering tend to cluster within the *FT* clade, while genes that repress flowering tend to cluster with the *TFL1* clade (Pin *et al.*, 2010; Bennett & Dixon, 2021; Liu *et al.*, 2023a). Our analysis showed *Z. marina* and *Z. muelleri* both have genes that cluster within the *FT* clade and *TFL1* clade, as well as one predicted *MFT* paralog each. While sequence similarity cannot confirm or predict gene function (Delaux *et al.*, 2019), our analysis suggest that the *Z. marina* genome may have several representatives of the same floral pathway genes that are conserved across angiosperms.

Four *ZmaPEBP* genes affect flowering phenotype in overexpression assays

As a first step towards investigating the function of the *ZmaPEBP* genes, we characterized their protein structure and function. The predicted open reading frames for all *ZmaPEBP* genes encode proteins with high similarity to *Arabidopsis* FT and TFL1 of *Arabidopsis* and rice Hd3a of *Oryza sativa* (Fig. 2a, Fig. S1). We also observe the conservation of key residues for FT function (Hanzawa *et al.*, 2005; Ho & Weigel, 2014), such as at position 85 where all genes show conservation relative to *Arabidopsis* FT and TFL (Y85 in FT, and H85 in TFL1).

To gain further insight into the function of each *ZmaPEBP* gene, we created transgenic overexpression *Arabidopsis* lines (Col-0) of each *ZmaPEBP* gene to investigate the effect of expression of each candidate gene on flowering *Arabidopsis*. We validated *ZmaPEBP* expression in the T_1 generation (Fig. S2). Of the thirteen *ZmaPEBP* genes screened, four demonstrated a strong effect on flowering time. Overexpression of *ZmaFT2* and *ZmaFT4* resulted in early flowering in *Arabidopsis* under LD conditions, compared to a *35S:GFP* control (Fig. 2b). Both genes are found in the *FT/TSF* clade in our phylogenetic analysis (Fig. 1). In homozygous transgenic lines, overexpression of *ZmaFT4* had a stronger effect on flowering time than *ZmaFT2* (Fig. 2c, Figure S3a). *ZmaFT9* and *ZmaTFL1a* lines showed delay in flowering time, with a much stronger phenotype observed in *ZmaFT9* lines in homozygous lines (Fig. 2b-c). *ZmaTFL1a* is in the *TFL/BFT* clade with *Arabidopsis TFL1*, while *ZmaFT9*, which has the stronger delay in flowering time, is found in the *FT/TSF* clade (Fig. 1). We also observed a decrease in *LFY* and *API*, downstream targets of *FT*, in homozygous *35S:ZmaFT9* and *35S:ZmaTFL1a* lines, indicating some effect on the *FT* pathway in *Arabidopsis* (Fig. S3b). Further, flowers produced on T_1 generation plants showed a morphological phenotype similar to *TFL* overexpression *Arabidopsis* plants and to mutant *lfy* plants where additional leaf-like structures develop in place of petals and floral organs (Huala & Sussex, 1992; Hanano & Goto, 2011) (Fig. S3c). Together, these results indicate that *Z. marina* has two *PEBP* genes that promote flowering and two that repress flowering, all of which do so through interaction with the floral pathway.

Genetic structure between annual and perennial ecotypes provides context for the potential roles of *ZmaPEBP* genes

To study the roles of *ZmaFT2*, *ZmaFT4*, *ZmaFT9*, and *ZmaTFL1a* in eelgrass flowering and shoot architecture in plants with varying genetic backgrounds, we analyzed gene expression in vegetative and flowering shoots across different natural populations. When eelgrass flowers, the vegetative shoot primarily made up of leaves originating at the shoot base produces a bolted stem with multiple inflorescences, completely changing the shoot architecture of the plant (Fig. 3a-d). We focused on sampling plants from eelgrass meadows with shoots undergoing both clonal and sexual reproduction at three perennial sites, and from meadows where sexual flowering is the predominant mode of reproduction at three annual sites (two within Willapa Bay and one in Yaquina Bay; Fig. 3e-g, Table S4).

To test whether population structure or life history type influenced expression patterns in *ZmaPEBP*, we estimated genetic distance and population structure across these five eelgrass meadows (Fig. 3e-g). Reduced representation sequencing (RAD-seq) identified 327 loci (single nucleotide polymorphisms; SNPs) across 224 individuals (Table S4). Tests for population structure (Fig. 3h, Fig. S4, Table S6) revealed significant genetic differentiation between life history types (annual and perennial), and, to a lesser extent, between geographic regions within ecotypes. Pairwise genetic distances ($F_{ST;}$ Table S6) were highest and significant for all pairwise comparisons between annual and perennial sites, including the co-located annual and perennial sites at Stackpole. Amongst the perennial populations, the Stackpole perennial population in the west of the Bay was significantly differentiated from the two populations in the east, but these distances were lower than between annual and perennial populations; however, there was no significant structure between the eastern populations, Bay Center and Long Island (Table S4). Small but significant genetic differentiation was also observed between the annual sites, Stackpole annual in the north and Nahcotta Port in the south (Table S4). Similarly, DAPC analyses (Fig. S4b) separated annual from perennial populations on the first axis (explaining 71.3% of the variation in the data set) and both north-south (annual sites) and east-west (perennial sites) geographic structure on the second axis (12.3% of the variation). Finally, tests for individual population assignment revealed two primary clusters ($K = 2$), explained primarily by the assignment of most individuals in the annual population one group, and those from perennial populations to the second group (Fig. S4A). Overall, population structure across ecotypes, as well as across small geographic distances within ecotypes, (less than 20km in a single bay) allowed us to test for common gene expression patterns associated with flowering.

Finally, we also included annual samples from Yaquina Bay (Table S4), 140 km to the south and likely genetically distinct (Yu *et al.*, 2023) in the expression analyses.

Expression of *ZmaPEBP* genes changes across development and tissue type

To gain insight into the roles of *ZmaFT2*, *ZmaFT4*, *ZmaFT9*, and *ZmaTFL1a* in eelgrass flowering, shoot architecture and development, we analyzed gene expression in different tissues from both adult vegetative and flowering shoots from each perennial population (Fig. 4a-b, Table S4). In *Z. marina*, the two flowering activators, *ZmaFT2* and *ZmaFT4* (Fig. 2b-c), had higher expression in stem and rhizome of flowering compared to vegetative shoots, but expression in leaves was more similar between life stages (Fig. 4b, Fig. S5, Table S7). Although *ZmaTFL1a* acted as a flowering repressor when overexpressed in *Arabidopsis* (Fig. 2b-c), its expression decreased in flowering tissue relative to vegetative shoots, whereas expression in stem and rhizome tissue increased in flowering relative to vegetative shoots (Fig. 4a-b). This result was surprising, since the shoot apical meristem of the plant was in the vegetative stem tissue section, and expression was observed in tissues beyond the shoot apical meristem, where *TFL1* expression is typically found in other plant species (Bradley *et al.*, 1997; Ratcliffe *et al.*, 1999; Nakagawa *et al.*, 2002; MacAlister *et al.*, 2012). Both *ZmaFT4* and *ZmaTFL1a* showed significantly higher levels of expression in the tip of vegetative leaves compared to other sections of vegetative leaves (Fig. S5, Table S8). These spatial distribution patterns within the leaves resembled that of *FT* in *Arabidopsis* (Takada & Goto, 2003). The expression levels of the other floral repressor, *ZmaFT9* (Fig. 2b-c), were lower in leaves and stems from flowering shoots compared to vegetative shoots (Fig. 4a-b, Fig. S5, Table S3). Together, these results suggest that *ZmaFT9* correlates to the vegetative state in eelgrass adult perennials.

Our results in *Z. marina* highlight the expression of floral activators in stem and rhizome tissue, a pattern not observed in *Arabidopsis*. *ZmaTFL1a*, contrary to its apparent function as a floral repressor in *Arabidopsis*, is upregulated in stem and rhizome flowering tissue. However, *TFL1* is known to also play a role in shoot architecture and development in *Arabidopsis* (Shannon & Meeks-Wagner, 1991; Kobayashi *et al.*, 1999), which aligns with our observed expression in flowering stems. Overall, our results suggest that *ZmaFT2*, *ZmaFT4*, *ZmaFT9*, and *ZmaTFL1a* are implicated in eelgrass floral development and show tissue-specific expression patterns.

Expression of *ZmaPEBP* genes changes over the lifecycle of an annual ecotype

Due to the annual ecotype's predictability of flowering, annuals provide a system in which to study *PEBP* gene expression trends over the development of the plant throughout the growing season and their relationship to flowering onset. To this end, we characterized expression of *ZmaFT2*, *ZmaFT4*, *ZmaFT9*, and *ZmaTFL1a* at different time points across the growing season from two annual populations in Willapa Bay (Stackpole Annual and Nahcotta Port Annual, Fig. 3h). In the 2023 season in Willapa Bay, seedlings at these sites emerged in early April, and differentiation to flowering occurred in late June (Fig. 5a, Fig. S6). The emergence of flowering shoots coincides with peak photoperiod (approximately 16 hours, Fig. 5b).

In both *ZmaFT2* and *ZmaFT4*, we observed increasing expression over the season, with a more significant increase occurring when flowering shoots emerged (Fig. 5c, Fig. S7, Table S9, Table S10). This trend was far more apparent in root and rhizome tissue than in leaf tissue, though there was a marked increase in leaf tissue gene-expression on 19 Jun 2023 (Julian Date 23170) in ST-ANN and 6 Jul 2023 (Julian Date 23187) in NP-ANN, just as bolted flowering shoots were observed, which dissipated by the next time point. A similar trend was observed in *ZmaTFL1a* expression, with slight increased expression in leaves just as flowering shoots emerged and a general increase in expression after flowering shoots emerged, primarily in roots and rhizomes (Fig. S7). These results align with expression trends observed in perennial shoots (Fig. 4b). The peak in *ZmaFT2*, *ZmaFT4*, and *ZmaTFL1a* leaf expression also coincides with the maximum photoperiod (Fig. 5b). *ZmaFT9*, unlike the other *ZmaPEBP* genes, is expressed at higher levels in leaves at earlier stages of vegetative development. Approximately one month before flowering shoots were observed, we saw a decrease in expression (Fig. 5c). The average daily temperature rose 3°C (12°C to 15°C) and 1.9°C (14.9°C to 16.8°C) between 9 May 2023 (23129) and 18 May 2023 (23138) during this interval at ST-ANN and NP-ANN, respectively, with daily maxima ranging from 18°C to 29.5°C at ST-ANN and 17°C to 25.5°C at NP-ANN (Fig. 5d-e). The large decline in *ZmaFT9* expression was followed by a slower decline in expression after flowering shoots emerged. These results also align with tissue and developmental state-specific expression trends observed in perennial shoots (Fig. 4b). We also analyzed expression levels of *ZmFT2*, *ZmFT4*, *ZmFT9*, and *ZmTFL1a* in annuals from Yaquina

Bay (YQ-ANN, Table S4). Trends in expression of each gene align with expression patterns observed in ST-ANN and NP-ANN site (Fig. S8) however results from YQ-ANN were either not statistically significant or less significant, likely due to limited sample size size and sampling of clonal branches rather than bolting portions (Table S11 and S12).

Together, these results suggest that *ZmaFT2* and *ZmaFT4* are involved in the activation of flowering, potentially in the formation of floral meristems and inflorescences, with *ZmaTFL1a* involved in some shoot architecture function after the flowering shoot has bolted. *ZmaFT9*, on the other hand, is seemingly involved with vegetative growth and development, and appears to require a decrease in expression to allow flowering onset to occur.

DISCUSSION

In this study, we aimed to characterize florigen genes in eelgrass and to examine their function in regulating the onset of flowering. The molecular controls and regulatory mechanisms for the onset of flowering in *Z. marina* have not been previously investigated, despite the importance of sexual reproduction in improving resiliency in populations, a key goal for restoration efforts (Kendrick *et al.*, 2012). Identifying and characterizing flowering genes and their effect on flowering onset in eelgrass will inform how flowering may be cued in eelgrass and how eelgrass is predicted to sexually reproduce under climate change conditions.

Here, we provide evidence of functional *FT/TFL1* homologs in *Z. marina*, with both activating and repressing function in flowering. We identify thirteen florigen homologous genes in eelgrass and demonstrate that four are functionally relevant to the flowering pathway. We show that *Z. marina*, like other monocots, has an expanded *FT* clade within the *PEBP* gene family, which is also mirrored in *Z. marina*'s sister species, *Z. muelleri*. Using *Arabidopsis* to assess the function of *Z. marina PEPB* genes, we demonstrate that overexpression of four *ZmaPEBP* genes results in either precocious flowering (*ZmaFT2* and *ZmaFT4*) or delayed flowering (*ZmaFT9* and *ZmTFL1a*). To the best of our knowledge, these results provide the first functional implication of florigen in marine angiosperms. Further, we observed tissue-specific expression patterns of these *ZmaPEBP* genes that correlate to developmental state (flowering and vegetative) in both annual and perennial *Z. marina* shoots. We believe that the role of the four focal genes (*ZmaFT2*, *ZmaFT4*, *ZmaFT9*, and *ZmaTFL1a*) is conserved across annual and perennial ecotypes, and across geographically structured populations, based on the similarity of

gene expression patterns (Fig. 4 and 5). Our findings add to the expanding body of knowledge on seasonal flowering through the balance of floral activators and repressors and bring new insight into *FT*-flowering pathway function beyond terrestrial plants and model and crop species.

Z. marina **harbors a large expansion of *FT* genes with *ZmaFT2* and *ZmaFT4* likely contributing to flowering onset**

In *Arabidopsis*, there are six *PEBP* genes (*FT*, *TSF*, *TFL1*, *ATC*, *BFT*, and *MFT*), with *FT* as the main inducer of flowering and *TSF* with redundant functionality. Our phylogenetic analysis demonstrated an expansion in the *PEBP* gene family focused within the *FT* clade. Ten of the thirteen *ZmaPEBP* genes identified fell within *FT/TSF* clade, consistent with the phylogenetic analysis of *FT* genes described in Liu et al. (Liu *et al.*, 2023a). Further completion and annotation of the *Z. marina* genome may reveal other florigen genes as well as insights into other genes implicated in flowering processes. In eelgrass, *ZmaFT2* and *ZmaFT4* likely contribute to the activation of flowering in a manner similar to *FT* and are apparent drivers of flowering. Interestingly, *ZmaFT1*, the closest related paralog to *ZmaFT2*, shows no flowering phenotype when overexpressed in *Arabidopsis* (Fig. 2b). We speculate that this lack of apparent flowering function in *Arabidopsis* may be due to a mutation in ZmaFT1 at a key amino acid residue, Q140 (Ho & Weigel, 2014), which is a histidine (H) in ZmaFT1 rather than a glutamine (Q) but is conserved in both ZmaFT2 and ZmaFT4 (Fig. 2a). Gln140 forms hydrogen bonds with Tyr85 (Y85), another important residue (Hanzawa *et al.*, 2005; Ho & Weigel, 2014), conserved in all ZmaFT homologs within the FT clade. In wild populations, both *ZmaFT2* and *ZmaFT4* show increased expression in stem and rhizome tissue after the onset of flowering in both perennial and annual shoots. Further, there is a slight increase in expression observed in leaf tissue just before the emergence of flowering shoots. This peak in expression in annual populations approximately coincided with maximum photoperiod, indicating that photoperiod may be one influencing factor on the expression of these *ZmaFT* genes. This result coincides with previous literature, where temperature, salinity, and photoperiod were found as environmental controls of flowering (McMillan, 1976; Harwell & Rhode, 2007; Blok *et al.*, 2018).

***ZmaFT9* may be the main determinant of flowering through repression of flowering function**

Despite the importance of activators within the *PEBP* gene family and other plant species, our results suggest that a repressor, namely *ZmaFT9*, may play a role as a major determinant of flowering onset in *Z. marina*. Not only did overexpression of *ZmaFT9* have a significant delay in flowering time in *Arabidopsis*, but its expression was also restricted to vegetative leaves in both the annual and perennial populations in *Z. marina*. Moreover, *ZmaFT9* expression decreased sharply approximately one month before flowering shoots emerge in the annual ecotype. Only after *ZmaFT9* expression decreases do we observe increased expression in *ZmaFT2* and *ZmaFT4*, suggesting that they are likely activators of flowering. These results suggest the involvement of *ZmaFT9* in the repression of flowering and maintenance of the vegetative state. Given that *ZmaFT9* is found only in leaves, we hypothesize that *ZmaFT9* acts as an anti-florigen (Higuchi, 2018), which too is expressed in the leaves like canonical *FT* (Takada & Goto, 2003) but prevents activation of flowering through repression of flower-activating gene expression, and ultimately is a major determinant of flowering onset on *Z. marina*. In this framework, the presence of antiflorigen maintains the vegetative state in shoots, and when it is substantially reduced, the shoot experiences the onset of flowering. Adult perennial shoots that remained vegetative during peak flowering time in the field express *ZmaFT9* at high levels, which was not seen in adult perennial flowering shoots (Fig. 4). High expression levels of *ZmaFT9* throughout the time of flowering onset may explain the low flowering frequency observed in perennial populations.

Most *PEBP* genes within the *FT* clade activate flowering in a similar manner to the florigen described originally in the 20th century, where a floral stimulus originates in the leaves and travels to the shoot meristem (Chailakhyan, 1937). However, a *FT* homolog that functions antagonistically to a canonical florigen is not completely novel. In onions (*Allium cepa*), *AcFT4* expression prevents bulb formation and when overexpressed in *Arabidopsis* significantly delays flowering (Lee *et al.*, 2013). *BvFT1* in beets (*Beta vulgaris*) represses flowering through repression of *BvFT2*, the functionally conserved homolog of *FT* in *Arabidopsis* (Pin *et al.*, 2010). Similarly, chrysanthemums (*Chrysanthemum seticuspe*) also contain an antiflorigenic FT/TFL1 family protein (CsAFT) that acts antagonistically to CsFTL3 (Higuchi *et al.*, 2013). *ZmaFT9* is likely the first antiflorigen to be described in a marine angiosperm where clonal propagation

maintains meadows. Further study revealing the mechanism of repression will provide insights into the evolution of the strategy by which *Z. marina* and other marine angiosperms regulate flowering.

***ZmaTFL1a* may play a role in regulating flowering shoot architecture and other processes not related to flowering**

While many genes that group within the *FT* or *TFL1* clade have previously described function in regulating flowering, we know that several *PEBP* genes are implicated in developmental processes other than flowering (Wickland & Hanzawa, 2015). In strawberries (*Fragaria vesca*), three *FT* genes collectively impact plant architecture and *FveFT3* has a strong effect on fruit yield (Gaston *et al.*, 2021). The *FT* homolog *StSP6A* induced tuberization in potato (*Solanum tuberosum*) (Navarro *et al.*, 2011). In addition, other genes and transcription factors can interact with *FT* homologs to regulate various processes, such as *BRANCHED1* (*BRC1*), which interacts with *FT* to suppress floral development in axillary meristems (Niwa *et al.*, 2013). *TFL1* homologs are also known to play a role in flowering shoot architecture, with *tfl1* *Arabidopsis* plants having short stems with single terminal flowers (Shannon & Meeks-Wagner, 1991; Kobayashi *et al.*, 1999). Overexpression of *RCN1* and *RCN2*, the *TFL1* homologs in rice (*Oryza sativa*) prevents stem elongation and affects branching and panicle development in rice plants (Nakagawa *et al.*, 2002). *ZmaTFL1a* appears to be either not expressed or expressed at low levels in leaf tissue in vegetative perennial shoots (Fig. 4). In both ecotypes, *ZmaTFL1a* expression increases greatly in rhizome tissue once the floral transition has occurred (Fig. 7 and S7). Paired with the delayed flowering phenotype in *35S:ZmaTFL1a Arabidopsis* (Fig. 2), we hypothesize that *ZmaTFL1a* may play a role in flowering shoot architecture and regulate spathe and inflorescence formation. Further study of *ZmaTFL1a* function and regulation within *Z. marina* populations may yield new insights into increasing seed potential in a population, a key component of increasing population genetic diversity (Kendrick *et al.*, 2012) and a strategy currently being used in restoration practices in the eastern United States (Marion & Orth, 2010; Orth *et al.*, 2012, 2020).

With further study of the *Z. marina* genome and transcriptome analyses, we expect that other genes related to flowering will be identified and characterized. We also expect that additional study and transcriptomic analyses will reveal insights into the potential functions of

the other *ZmaPEBP* candidate genes that were not brought to light by this study due to experimental limitations and lack of genetics and gene-editing tools. Our study focused primarily on flowering onset and therefore did not pursue inquiry in other developmental functions. However, given the wide array of effects the expression of these genes has on various developmental processes in other plant species, we expect that future studies will further elucidate the roles of *PEBP* genes in eelgrass. We also expect that further study of activating and repressing florigens in the context of different eelgrass population and sites on a larger scale will provide more insights to how these genes impact reproduction- and restoration-focused research. Given our environmental conditions, we predict that the timing and regulation of *ZmaPEBP* genes is affected by local environmental conditions and suggest that continued research into the role of *ZmaPEBP* genes in flowering will allow for more strategic and efficient seed-based restoration efforts of eelgrass.

CONCLUSION

Our study begins to address the long-standing question of why certain eelgrass shoots flower in a given season and why flowering frequency varies across spatial scales and seasonally. There is a breadth of work exploring this question from the population level, often comparing local environmental factors (Phillips *et al.*, 1983; Yang *et al.*, 2013; Blok *et al.*, 2018; von Staats *et al.*, 2021; Ruesink *et al.*, 2022), but no studies to date approaching this question from a molecular and mechanistic perspective. Rising atmospheric and water temperatures and increasing frequency of extreme climate events predicted as a result of climate change will likely increase the thermal stress on marine and aquatic ecosystems and have impacts on eelgrass population health (Hobday *et al.*, 2018; Jager *et al.*, 2018; Kendrick *et al.*, 2019). With global loss of seagrass populations estimated at 7% annually and rising (Orth *et al.*, 2006; Waycott *et al.*, 2009) and given the importance of seeds in promoting resiliency in eelgrass populations (Kendrick *et al.*, 2012), a key gap has been understanding how climate change and warming events will impact eelgrass reproduction and persistence. Characterization of the interacting genetic by environmental controls of flowering will lead to a better understanding of factors affecting seed production and to improved seed-based restoration strategies. Understanding how local climate and environmental stimuli affect plant reproductive processes may provide insight

617 into how populations will respond to climate change and help inform their restoration and
618 management.
619
620 **ACKNOWLEDGEMENTS**
621 We thank A. K. Hempton, W. Albers, C. Nguyen, K. Kranzler, and A. Keely for technical support
622 and assistance. This research was funded by Washington State Department of Natural Resources
623 Interagency Agreements (93-102930 to J. L. R. and T. I.., and 93-106455 to T. I.), U.S.
624 Geological Survey Northwest Climate Adaptation Science Center award G17AC00218 to C. T.
625 N., the University of Washington Biology Department (W. T. Edmonson Award, Lawrence Giles
626 Botanical Field Research Award, and the Kruckeberg-Walker Award to C. T. N., and the Frye-
627 Hotson Rigg Award to I. C.), and in part by the National Institute of Health (R01GM079712 to
628 T.I.). The views expressed in this article are those of the authors and do not necessarily represent
629 the views or policies of the U.S. Environmental Protection Agency.
630
631 **COMPETING INTERESTS**
632 The authors declare no competing interest.
633
634 **AUTHOR CONTRIBUTIONS**
635 C. T. N, C. D., J. L. R., and T. I. designed the research. C. T. N., I. C., A. F.-S., and B. A. B. O.
636 performed research. C. T. N., I. C., A. F.-S., B. A. B. O., K. A. N., V. D. S., J.E.K., and J. L. R.
637 analyzed, collected, and/or interpreted data. C. T. N, I. C., J. L. R., and T. I. obtained funding. C.
638 T. N., B. A. B. O., K. A. N., J. L. R., and T. I. wrote the manuscript, together with all authors'
639 contribution.
640
641 **DATA AVAILABILITY**
642 All alignments, scripts, population metadata, and genotypes (filtered and unfiltered) will be
643 available on Dryad at the following link upon acceptance.
644 https://doi.org/10.5061/dryad.sbcc2frh0
645

646 **REFERENCES:**
647
648 **Ali OA, O'Rourke SM, Amish SJ, Meek MH, Luikart G, Jeffres C, Miller MR**. **2016**. RAD
649 Capture (Rapture): Flexible and efficient sequence-based genotyping. *Genetics* **202**: 389–400.

650 **Altschul SF, Gish W, Miller W, Myers EW, Lipman DJ**. **1990**. Basic local alignment search
651 tool. *Journal of Molecular Biology* **215**: 403–410.

652 **Astronomical Applications Department, U. S. Naval Observatory**. **2023**. Duration of
653 Daylight/Darkness Table for One Year.

654 **Balasubramanian S, Sureshkumar S, Lempe J, Weigel D**. **2006**. Potent induction of
655 *Arabidopsis thaliana* flowering by elevated growth temperature. *PLOS Genetics* **2**: e106.

656 **Bates D, Mächler M, Bolker B, Walker S**. **2015**. Fitting linear mixed-effects models using
657 lme4. *Journal of Statistical Software* **67**: 1–48.

658 **Baumann K, Venail J, Berbel A, Domenech MJ, Money T, Conti L, Hanzawa Y, Madueno**
659 **F, Bradley D**. **2015**. Changing the spatial pattern of *TFL1* expression reveals its key role in the
660 shoot meristem in controlling *Arabidopsis* flowering architecture. *Journal of Experimental*
661 *Botany* **66**: 4769–4780.

662 **Bennett T, Dixon LE**. **2021**. Asymmetric expansions of FT and TFL1 lineages characterize
663 differential evolution of the EuPEBP family in the major angiosperm lineages. *BMC Biology* **19**:
664 181.

665 **Blázquez MA, Ahn JH, Weigel D**. **2003**. A thermosensory pathway controlling flowering time
666 in *Arabidopsis thaliana*. *Nature Genetics* **33**: 168–171.

667 **Blok SE, Olesen B, Krause-Jensen D**. **2018**. Life history events of eelgrass *Zostera marina L.*
668 populations across gradients of latitude and temperature. *Marine Ecology Progress Series* **590**:
669 79–93.

670 **Bradley D, Ratcliffe O, Vincent C, Carpenter R, Coen E**. **1997**. Inflorescence commitment
671 and architecture in *Arabidopsis*. *Science* **275**: 80–83.

672 **Briones Ortiz B, Boardman FC, Ruesink JL, Naish KA**. ***In press***. Adaptive genetic
673 differentiation between spatially proximate annual and perennial life history types of a marine
674 foundation species. *Molecular Ecology*.

675 **Catchen J, Hohenlohe PA, Bassham S, Amores A, Cresko WA**. **2013**. Stacks: an analysis tool
676 set for population genomics. *Molecular Ecology* **22**: 3124–3140.

677 **Chailakhyan MK**. **1937**. Concerning the hormonal nature of plant development processes.
678 *Doklady Akademii Nauk SSSR* **16**: 227–230.

679 **Chang CC, Chow CC, Tellier LC, Vattikuti S, Purcell SM, Lee JJ**. **2015**. Second-generation
680 PLINK: rising to the challenge of larger and richer datasets. *Gigascience* **4**: 7.

Corbesier L, Vincent C, Jang S, Fornara F, Fan Q, Searle I, Giakountis A, Farrona S, Gissot L, Turnbull C, *et al.* 2007. FT protein movement contributes to long-distance signaling in floral induction of *Arabidopsis*. *Science* **316**: 1030–1033.

Cronau RJT, de Fouw J, van Katwijk MM, Bouma TJ, Heusinkveld JHT, Hoeijmakers D, Lamers LPM, van der Heide T. 2023. Seed- versus transplant-based eelgrass (*Zostera marina L.*) restoration success in a temperate marine lake. *Restoration Ecology* **31**: e13786.

Delaux P-M, Hetherington AJ, Coudert Y, Delwiche C, Dunand C, Gould S, Kenrick P, Li F-W, Philippe H, Rensing SA, *et al.* 2019. Reconstructing trait evolution in plant evo–devo studies. *Current Biology* **29**: R1110–R1118.

DeRaad DA. 2022. snpfiltr: An R package for interactive and reproducible SNP filtering. *Molecular Ecology Resouces* **22**: 2443–2453.

Duffy JE, Stachowicz JJ, Reynolds PL, Hovel KA, Jahnke M, Sotka EE, Boström C, Boyer KE, Cusson M, Eklöf J, *et al.* 2022. A Pleistocene legacy structures variation in modern seagrass ecosystems. *Proceedings of the National Academy of Sciences* **119**: e2121425119.

Evanno G, Regnaut S, Goudet J. 2005. Detecting the number of clusters of individuals using the software structure: a simulation study. *Molecular Ecology* **14**: 2611–2620.

Gaston A, Potier A, Alonso M, Sabbadini S, Delmas F, Tenreira T, Cochetel N, Labadie M, Prévost P, Folta KM, *et al.* 2021. The FveFT2 florigen/FveTFL1 antiflorigen balance is critical for the control of seasonal flowering in strawberry while FveFT3 modulates axillary meristem fate and yield. *New Phytologist* **232**: 372–387.

Goudet J. 2005. hierfstat, a package for r to compute and test hierarchical F-statistics. *Molecular Ecology Notes* **5**: 184–186.

Hanano S, Goto K. 2011. *Arabidopsis* TERMINAL FLOWER1 is involved in the regulation of flowering time and inflorescence development through transcriptional repression. *The Plant Cell* **23**: 3172–3184.

Hanzawa Y, Money T, Bradley D. 2005. A single amino acid converts a repressor to an activator of flowering. *Proceedings of the National Academy of Sciences* **102**: 7748–7753.

Harwell MC, Rhode JM. 2007. Effects of edge/interior and patch structure on reproduction in *Zostera marina* L. in Chesapeake Bay, USA. *Aquatic Botany* **87**: 147–154.

Hays CG, Hanley TC, Hughes AR, Truskey SB, Zerebecki RA, Sotka EE. 2021. Local adaptation in marine foundation species at microgeographic scales. *The Biological Bulletin* **241**: 16–29.

Hickey BM, Banas NS. 2003. Oceanography of the U.S. Pacific Northwest Coastal Ocean and estuaries with application to coastal ecology. *Estuaries* **26**: 1010–1031.

Higuchi Y. **2018**. Florigen and anti-florigen: flowering regulation in horticultural crops. *Breeding Science* **68**: 109–118.

Higuchi Y, Narumi T, Oda A, Nakano Y, Sumitomo K, Fukai S, Hisamatsu T. **2013**. The gated induction system of a systemic floral inhibitor, antiflorigen, determines obligate short-day flowering in chrysanthemums. *Proceedings of the National Academy of Sciences* **110**: 17137–17142.

Ho WWH, Weigel D. **2014**. Structural features determining flower-promoting activity of *Arabidopsis* FLOWERING LOCUS T. *The Plant Cell* **26**: 552–564.

Hoang DT, Chernomor O, von Haeseler A, Minh BQ, Vinh LS. **2018**. Ufboot2: improving the ultrafast bootstrap approximation. *Molecular Biology and Evolution* **35**: 518–522.

Hobday AJ, Oliver ECJ, Gupta AS, Benthuysen JA, Burrows MT, Donat MG, Holbrook NJ, Moore PJ, Thomsen MS, Wernberg T, *et al.* 2018. Categorizing and naming marine heatwaves. *Oceanography* **31**: 162–173.

Huala E, Sussex IM. **1992**. LEAFY interacts with floral homeotic genes to regulate Arabidopsis floral development. *The Plant Cell* **4**: 901–913.

Itoh H, Nonoue Y, Yano M, Izawa T. **2010**. A pair of floral regulators sets critical day length for *Hd3a* florigen expression in rice. *Nature Genetics* **42**: 635–638.

Jager HI, King AW, Gangrade S, Haines A, DeRolph C, Naz BS, Ashfaq M. **2018**. Will future climate change increase the risk of violating minimum flow and maximum temperature thresholds below dams in the Pacific Northwest? *Climate Risk Management* **21**: 69–84.

Jombart T, Ahmed I. **2011**. adegenet 1.3-1: new tools for the analysis of genome-wide SNP data. *Bioinformatics* **27**: 3070–3071.

Kalyaanamoorthy S, Minh BQ, Wong TKF, von Haeseler A, Jermiin LS. **2017**. ModelFinder: fast model selection for accurate phylogenetic estimates. *Nature Methods* **14**: 587–589.

Kardailsky I, Shukla VK, Ahn JH, Dagenais N, Christensen SK, Nguyen JT, Chory J, Harrison MJ, Weigel D. **1999**. Activation tagging of the floral inducer *FT*. *Science* **286**: 1962–1965.

Karimi M, Inzé D, Depicker A. **2002**. GATEWAY™ vectors for *Agrobacterium*-mediated plant transformation. *Trends in Plant Science* **7**: 193–195.

Katoh K, Misawa K, Kuma K, Miyata T. **2002**. MAFFT: a novel method for rapid multiple sequence alignment based on fast Fourier transform. *Nucleic Acids Research* **30**: 3059–3066.

van Katwijk MM, Thorhaug A, Marbà N, Orth RJ, Duarte CM, Kendrick GA, Althuizen IHJ, Balestri E, Bernard G, Cambridge ML, *et al.* 2016. Global analysis of seagrass restoration: the importance of large-scale planting. *Journal of Applied Ecology* **53**: 567–578.

Keddy CJ. **1987**. Reproduction of annual eelgrass: Variation among habitats and comparison with perennial eelgrass (*Zostera marina* L.). *Aquatic Botany* **27**: 243–256.

Kendrick GA, Nowicki RJ, Olsen YS, Strydom S, Fraser MW, Sinclair EA, Statton J, Hovey RK, Thomson JA, Burkholder DA, *et al.* 2019. A systematic review of how multiple stressors from an extreme event drove ecosystem-wide loss of resilience in an iconic seagrass community. *Frontiers in Marine Science* **6**: 455.

Kendrick GA, Waycott M, Carruthers TJB, Cambridge ML, Hovey R, Krauss SL, Lavery PS, Les DH, Lowe RJ, Vidal OM i, *et al.* 2012. The central role of dispersal in the maintenance and persistence of seagrass populations. *BioScience* **62**: 56–65.

Kinmonth-Schultz HA, Tong X, Lee J, Song YH, Ito S, Kim S-H, Imaizumi T. **2016**. Cool night-time temperatures induce the expression of *CONSTANS* and *FLOWERING LOCUS T* to regulate flowering in *Arabidopsis*. *New Phytologist* **211**: 208–224.

Kobayashi Y, Kaya H, Goto K, Iwabuchi M, Araki T. **1999**. A pair of related genes with antagonistic roles in mediating flowering signals. *Science* **286**: 1960–1962.

Kojima S, Takahashi Y, Kobayashi Y, Monna L, Sasaki T, Araki T, Yano M. **2002**. *Hd3a*, a rice ortholog of the *Arabidopsis FT* gene, promotes transition to flowering downstream of *Hd1* under short-day conditions. *Plant and Cell Physiology* **43**: 1096–1105.

Lee R, Baldwin S, Kenel F, McCallum J, Macknight R. **2013**. *FLOWERING LOCUS T* genes control onion bulb formation and flowering. *Nature Communications* **4**: 2884.

Lee H, Golicz AA, Bayer PE, Jiao Y, Tang H, Paterson AH, Sablok G, Krishnaraj RR, Chan C-KK, Batley J, *et al.* 2016. The genome of a southern hemisphere seagrass species (*Zostera muelleri*). *Plant Physiology* **172**: 272–283.

Lee JH, Yoo SJ, Park SH, Hwang I, Lee JS, Ahn JH. **2007**. Role of *SVP* in the control of flowering time by ambient temperature in *Arabidopsis*. *Genes & Development* **21**: 397–402.

Li H. **2013**. Aligning sequence reads, clone sequences and assembly contigs with BWA-MEM. *arXiv [q-bio.GN]*.

Lifschitz E, Ayre BG, Eshed Y. **2014**. Florigen and anti-florigen – a systemic mechanism for coordinating growth and termination in flowering plants. *Frontiers in Plant Science* **5**: 465.

Liu H, Liu X, Chang X, Chen F, Lin Z, Zhang L. **2023a**. Large-scale analyses of angiosperm *Flowering Locus T* genes reveal duplication and functional divergence in monocots. *Frontiers in Plant Science* **13**: 1039500.

Liu T-S, Wu K-F, Jiang H-W, Chen K-W, Nien T-S, Bryant DA, Ho M-Y. **2023b**. Identification of a far-red light-inducible promoter that exhibits light intensity dependency and reversibility in a cyanobacterium. *ACS Synthetic Biology* **12**: 1320–1330.

Ma X, Olsen JL, Reusch TBH, Procaccini G, Kudrna D, Williams M, Grimwood J, Rajasekar S, Jenkins J, Schmutz J, *et al.* 2021. Improved chromosome-level genome assembly and annotation of the seagrass, *Zostera marina* (eelgrass). *F1000Res.* **10**: 289.

MacAlister CA, Park SJ, Jiang K, Marcel F, Bendahmane A, Izkovich Y, Eshed Y, Lippman ZB. 2012. Synchronization of the flowering transition by the tomato TERMINATING FLOWER gene. *Nature Genetics* **44**: 1393–1398.

Maddison WP, Maddison DR. 2023. Mesquite: a modular system for evolutionary analysis.

Madeira F, Madhusoodanan N, Lee J, Eusebi A, Niewielska A, Tivey ARN, Lopez R, Butcher S. 2024. The EMBL-EBI Job Dispatcher sequence analysis tools framework in 2024. *Nucleic Acids Research* **52**: W521–W525.

Marion SR, Orth RJ. 2010. Innovative techniques for large-scale seagrass restoration using *Zostera marina* (eelgrass) seeds. *Restoration Ecology* **18**: 514–526.

McMillan C. 1976. Experimental studies on flowering and reproduction in seagrasses. *Aquatic Botany* **2**: 87–92.

de Meeûs T, Goudet J. 2007. A step-by-step tutorial to use HierFstat to analyse populations hierarchically structured at multiple levels. *Infection, Genetics and Evolution* **7**: 731–735.

Mimida N, Goto K, Kobayashi Y, Araki T, Ahn JH, Weigel D, Murata M, Motoyoshi F, Sakamoto W. 2001. Functional divergence of the *TFL1*-like gene family in *Arabidopsis* revealed by characterization of a novel homologue. *Genes to Cells* **6**: 327–336.

de Montaigu A, Tóth R, Coupland G. 2010. Plant development goes like clockwork. *Trends in Genetics* **26**: 296–306.

Nakagawa M, Shimamoto K, Kyozuka J. 2002. Overexpression of *RCN1* and *RCN2*, rice *TERMINAL FLOWER 1/CENTRORADIALIS* homologs, confers delay of phase transition and altered panicle morphology in rice. *The Plant Journal* **29**: 743–750.

Navarro C, Abelenda JA, Cruz-Oró E, Cuéllar CA, Tamaki S, Silva J, Shimamoto K, Prat S. 2011. Control of flowering and storage organ formation in potato by FLOWERING LOCUS T. *Nature* **478**: 119–122.

Nejrup LB, Pedersen MF. 2008. Effects of salinity and water temperature on the ecological performance of *Zostera marina*. *Aquatic Botany* **88**: 239–246.

Nguyen LT, Schmidt HA, von Haeseler A, Bui MQ. 2014. IQ-TREE: a fast and effective stochastic algorithm for estimating maximum-likelihood phylogenies. **32**: 268–274.

Niwa M, Daimon Y, Kurotani K, Higo A, Pruneda-Paz JL, Breton G, Mitsuda N, Kay SA, Ohme-Takagi M, Endo M, *et al.* 2013. BRANCHED1 interacts with FLOWERING LOCUS T to repress the floral transition of the axillary meristems in *Arabidopsis*. *The Plant Cell* **25**: 1228–1242.

Oda A, Narumi T, Li T, Kando T, Higuchi Y, Sumitomo K, Fukai S, Hisamatsu T. 2012. *CsFTL3*, a chrysanthemum *FLOWERING LOCUS T*-like gene, is a key regulator of photoperiodic flowering in chrysanthemums. *Journal of Experimental Botany* **63**: 1461–1477.

Olsen JL, Rouzé P, Verhelst B, Lin Y-C, Bayer T, Collen J, Dattolo E, De Paoli E, Dittami S, Maumus F, *et al.* 2016. The genome of the seagrass *Zostera marina* reveals angiosperm adaptation to the sea. *Nature* **530**: 331–335.

Orth RJ, Carruthers TJB, Dennison WC, Duarte CM, Fourqurean JW, Heck KL, Hughes AR, Kendrick GA, Kenworthy WJ, Olyarnik S, *et al.* 2006. A global crisis for seagrass ecosystems. *BioScience* **56**: 987–996.

Orth RJ, Lefcheck JS, McGlathery KS, Aoki L, Luckenbach MW, Moore KA, Oreska MPJ, Snyder R, Wilcox DJ, Lusk B. 2020. Restoration of seagrass habitat leads to rapid recovery of coastal ecosystem services. *Science Advances* **6**: eabc6434.

Orth RJ, Moore KA, Marion SR, Wilcox DJ, Parrish DB. 2012. Seed addition facilitates eelgrass recovery in a coastal bay system. *Marine Ecology Progress Series* **448**: 177–195.

Phillips RC, Stewart Grant W, Peter McRoy C. 1983. Reproductive strategies of eelgrass (*Zostera marina* L.). *Aquatic Botany* **16**: 1–20.

Pin PA, Benlloch R, Bonnet D, Wremerth-Weich E, Kraft T, Gielen JJL, Nilsson O. 2010. An antagonistic pair of FT homologs mediates the control of flowering time in sugar beet. *Science* **330**: 1397–1400.

Pin PA, Nilsson O. 2012. The multifaceted roles of FLOWERING LOCUS T in plant development. *Plant, Cell & Environment* **35**: 1742–1755.

Pritchard JK, Stephens M, Donnelly P. 2000. Inference of Population Structure Using Multilocus Genotype Data. *Genetics* **155**: 945–959.

Qin L-Z, Kim SH, Song H-J, Suonan Z, Kim H, Kwon O, Lee K-S. 2020. Influence of regional water temperature variability on the flowering phenology and sexual reproduction of the seagrass Zostera marina in Korean coastal waters. *Estuaries and Coasts* **43**: 449–462.

R Core Team. 2024. A Language and Environment for Statistical Computing_.

Ransbotyn V, Reusch TBH. 2006. Housekeeping gene selection for quantitative real-time PCR assays in the seagrass *Zostera marina* subjected to heat stress. *Limnology and Oceanography: Methods* **4**: 367–373.

Ratcliffe OJ, Bradley DJ, Coen ES. 1999. Separation of shoot and floral identity in *Arabidopsis*. *Development* **126**: 1109–1120.

Robertson AI, Mann KH. 1984. Disturbance by ice and life-history adaptations of the seagrass *Zostera marina*. *Marine Biology* **80**: 131–141.

Rochette NC, Catchen JM. **2017**. Deriving genotypes from RAD-seq short-read data using Stacks. *Nature Protocols* **12**: 2640–2659.

Ruesink JL, Feist BE, Harvey CJ, Hong JS, Trimble AC, Wisehart LM. **2006**. Changes in productivity associated with four introduced species: ecosystem transformation of a 'pristine' estuary. *Marine Ecology Progress Series* **311**: 203–215.

Ruesink JL, Ortiz BAB, Mawson CH, Boardman FC. **2022**. Tradeoffs in life history investment of eelgrass *Zostera marina* across estuarine intertidal conditions. *Marine Ecology Progress Series* **686**: 61–70.

Searle SR, Speed FM, Milliken GA. **1980**. Population marginal means in the linear model: an alternative to least squares means. *The American Statistician*.

Shannon S, Meeks-Wagner DR. **1991**. A mutation in the arabidopsis *TFL1* gene affects inflorescence meristem development. *The Plant Cell* **3**: 877–892.

Song YH, Ito S, Imaizumi T. **2013**. Flowering time regulation: photoperiod- and temperature-sensing in leaves. *Trends in Plant Science* **18**: 575–583.

Song YH, Kubota A, Kwon MS, Covington MF, Lee N, Taagen ER, Laboy Cintrón D, Hwang DY, Akiyama R, Hodge SK, *et al.* 2018. Molecular basis of flowering under natural long-day conditions in *Arabidopsis*. *Nature Plants* **4**: 824–835.

von Staats DA, Hanley TC, Hays CG, Madden SR, Sotka EE, Hughes AR. **2021**. Intra-meadow variation in seagrass flowering phenology across depths. *Estuaries and Coasts* **44**: 325–338.

Susila H, Nasim Z, Ahn J. **2018**. Ambient temperature-responsive mechanisms coordinate regulation of flowering time. *International Journal of Molecular Sciences* **19**: 3196.

Takada S, Goto K. **2003**. TERMINAL FLOWER2, an Arabidopsis homolog of HETEROCHROMATIN PROTEIN1, counteracts the activation of *FLOWERING LOCUS T* by CONSTANS in the vascular tissues of leaves to regulate flowering time. *The Plant Cell* **15**: 2856–2865.

Takagi H, Hempton AK, Imaizumi T. **2023**. Photoperiodic flowering in *Arabidopsis*: Multilayered regulatory mechanisms of *CONSTANS* and the florigen *FLOWERING LOCUS T*. *Plant Communications* **4**: 100552.

Thom RM, Borde AB, Rumrill S, Woodruff DL, Williams GD, Southard JA, Sargeant SL. **2003**. Factors influencing spatial and annual variability in eelgrass (*Zostera marina* L.) meadows in Willapa Bay, Washington, and Coos Bay, Oregon, estuaries. *Estuaries* **26**: 1117–1129.

Waycott M, Duarte CM, Carruthers TJB, Orth RJ, Dennison WC, Olyarnik S, Calladine A, Fourqurean JW, Heck KL, Hughes AR, *et al.* 2009. Accelerating loss of seagrasses across the globe threatens coastal ecosystems. *Proceedings of the National Academy of Sciences* **106**: 12377–12381.

Weigel D, Glazebrook J. **2002**. *Weigel, D. and Glazebrook, J. (2002) Arabidopsis: a laboratory manual. Cold Spring Harbor Laboratory Press, New York.* Cold Spring Harbor, New York: Cold Spring Harbor Laboratory Press.

Weir BS, Cockerham CC. **1984**. Estimating F-Statistics for the analysis of population structure. *Evolution* **38**: 1358–1370.

Weng L, Bai X, Zhao F, Li R, Xiao H. **2016**. Manipulation of flowering time and branching by overexpression of the tomato transcription factor *SlZFP2*. *Plant Biotechnology Journal* **14**: 2310–2321.

Wickland DP, Hanzawa Y. **2015**. The *FLOWERING LOCUS T/TERMINAL FLOWER 1* gene family: functional evolution and molecular mechanisms. *Molecular Plant* **8**: 983–997.

Wu L, Liu D, Wu J, Zhang R, Qin Z, Liu D, Li A, Fu D, Zhai W, Mao L. **2013**. Regulation of *FLOWERING LOCUS T* by a MicroRNA in *Brachypodium distachyon*. *The Plant Cell* **25**: 4363–4377.

Xi W, Liu C, Hou X, Yu H. **2010**. *MOTHER OF FT AND TFL1* regulates seed germination through a negative feedback loop modulating ABA signaling in *Arabidopsis*. *The Plant Cell* **22**: 1733–1748.

Yamaguchi A, Kobayashi Y, Goto K, Abe M, Araki T. **2005**. *TWIN SISTER OF FT (TSF)* acts as a floral pathway integrator redundantly with *FT*. *Plant and Cell Physiology* **46**: 1175–1189.

Yang S, Wheat EE, Horwith MJ, Ruesink JL. **2013**. Relative impacts of natural stressors on life history traits underlying resilience of intertidal eelgrass (*Zostera marina L.*). *Estuaries and Coasts* **36**: 1006–1013.

Yoo SJ, Chung KS, Jung SH, Yoo SY, Lee JS, Ahn JH. **2010**. *BROTHER OF FT AND TFL1 (BFT)* has *TFL1*-like activity and functions redundantly with *TFL1* in inflorescence meristem development in Arabidopsis. *The Plant Journal* **63**: 241–253.

Yoo SY, Kardailsky I, Lee JS, Weigel D, Ahn JH. **2004**. Acceleration of flowering by overexpression of *MFT* (MOTHER OF FT AND TFL1). *Molecules and Cells* **17**: 95–101.

Yoshida A, Taoka K, Hosaka A, Tanaka K, Kobayashi H, Muranaka T, Toyooka K, Oyama T, Tsuji H. **2021**. Characterization of frond and flower development and identification of FT and FD genes from duckweed *Lemna aequinoctialis* Nd. *Frontiers in Plant Science* **12**: 697206.

Yu L, Khachaturyan M, Matschiner M, Healey A, Bauer D, Cameron B, Cusson M, Emmett Duffy J, Joel Fodrie F, Gill D, *et al.* 2023. Ocean current patterns drive the worldwide colonization of eelgrass (Zostera marina). *Nature Plants* **9**: 1207–1220.

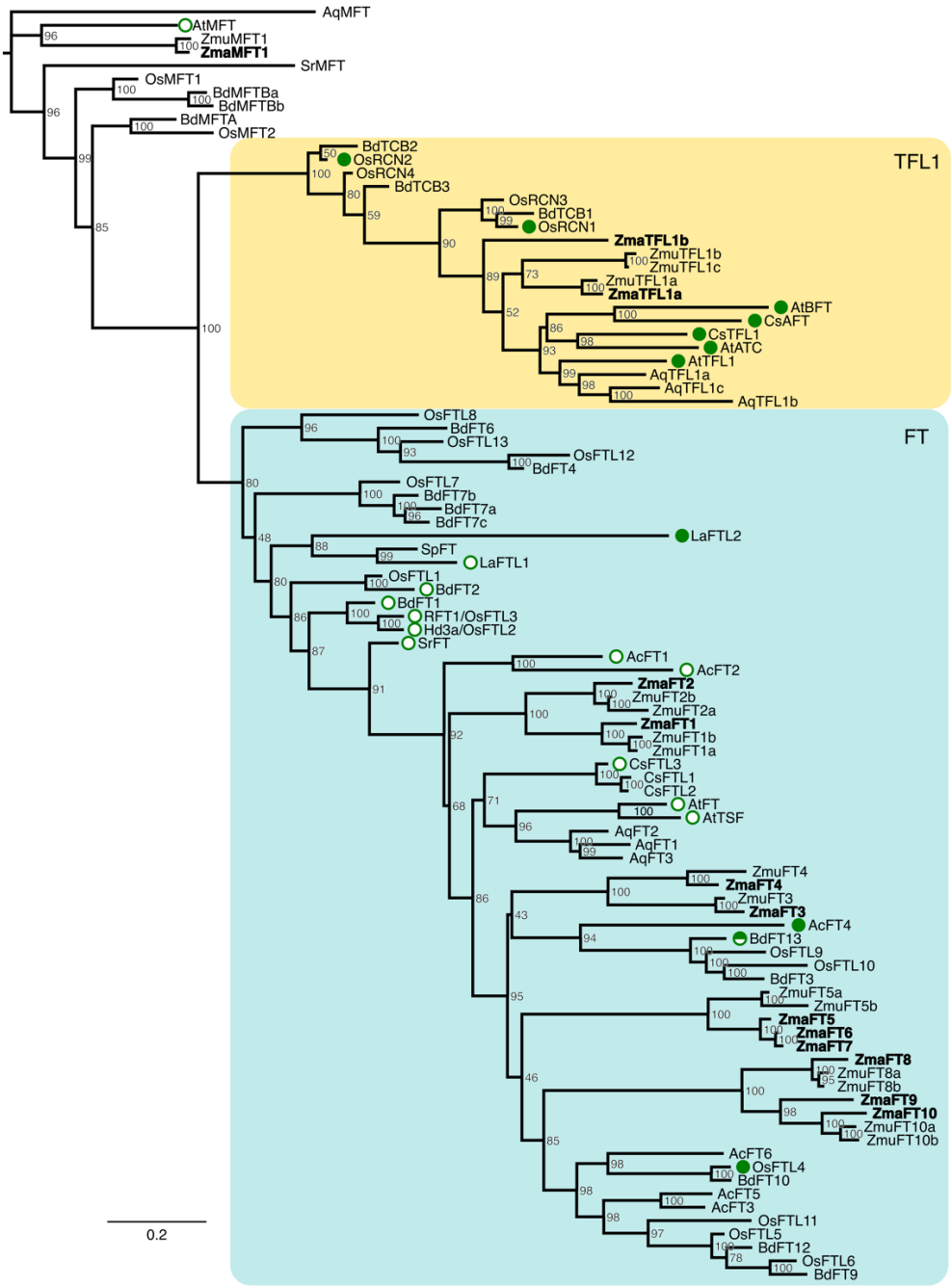

Figure 1: Phylogenetic tree of phosphatidylethanolamine binding protein (PEBP) genes in angiosperms. See Table S1 for sequence accession numbers. Nucleotide-level maximum likelihood analysis with 100 bootstraps, values shown at nodes. Species were chosen to represent the different angiosperm lineages having *PEBP* gene family members, with over-representation of monocotyledoneous and *Alismatales* taxa (monocotyledons: *B. distachyon, O. sativa*, *A. cepa*; *Alismatales*: *L. aequinoctialis, S. polyrhiza, S. renifolius, Z. marina, Z. muelleri;* other: *A. thaliana, A. coerulea, C. seticuspe*). *Z. marina* characterized here is shown in bold, and the tree includes its sister species *Z. muelleri* (*Zmu*). *PEBP* genes fall into two clades: *FT* (*FLOWERING LOCUS T,* blue) and *TFL1* (*TERMINAL FLOWER 1*, yellow). Open circles denote previously

934 described activators of flowering, closed circles denote repressors, and half-filled circle denotes
935 activator (under short-day conditions) and repressor (under long-day conditions).
936
937

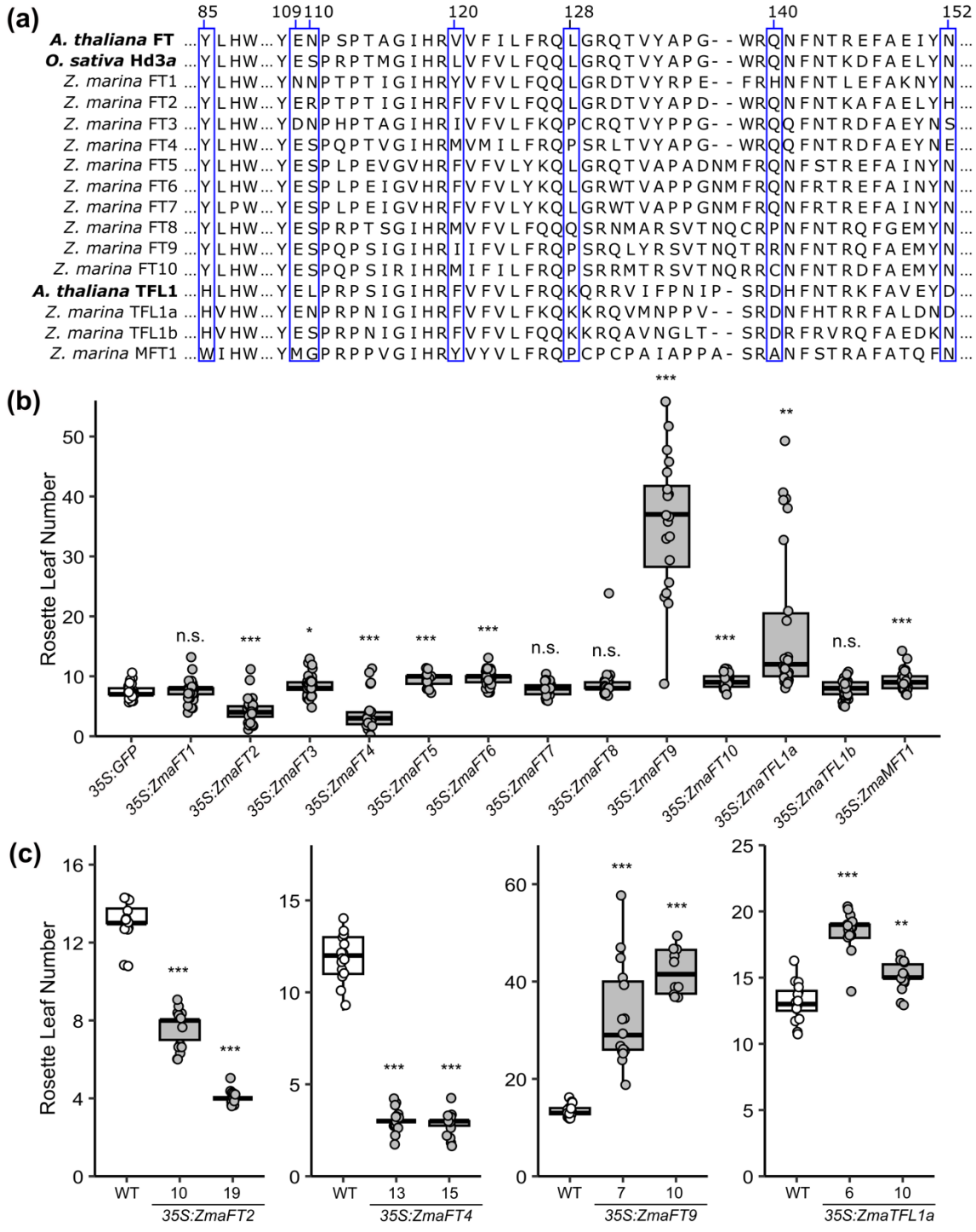

Figure 2: *ZmaFT* and *ZmaTFL1* genes alter flowering phenotype when overexpressed in *Arabidopsis thaliana.* **(a)** Amino acid sequence alignment of ZmaFT and ZmaTFL1 with *Arabidopsis thaliana* FT and TFL1 and *Oryza sativa* Hd3a (an FT ortholog). Blue boxes highlight residues important for FT function as a flowering promoter (blue). **(b)** Overexpression of thirteen *ZmaPEBP* orthologs under the control of the *35S* promoter highlighted four candidates that altered flowering time. *ZmaFT2* and *ZmaFT4* cause precocious flowering, while

946 *ZmaFT9* and *ZmaTFL1A* caused delayed flowering in the T_1 generation under long-day
947 conditions. Asterisks indicate significance based on t-test against the control (*35:GFP*), with
948 Bonferroni correction (n.s.: non-significant, *: $p < 0.0038$, **: $p < 0.00077$, ***: $p < 0.000077$).
949 **(c)** Altered flowering time phenotype was confirmed in homozygous individuals (T_3 generation).
950 Number labels on x-axis represent homozygous lines. Asterisks indicate significance based on t-
951 test comparing to wild type (WT) with Bonferroni correction (**: $p < 0.005$, ***: $p < 0.0005$).
952 All individuals are shown as data points (n≥16), with median indicated by center line in box,
953 upper and lower quartile by box boundaries, and highest and lowest value within two
954 interquartile ranges by whiskers.
955
956

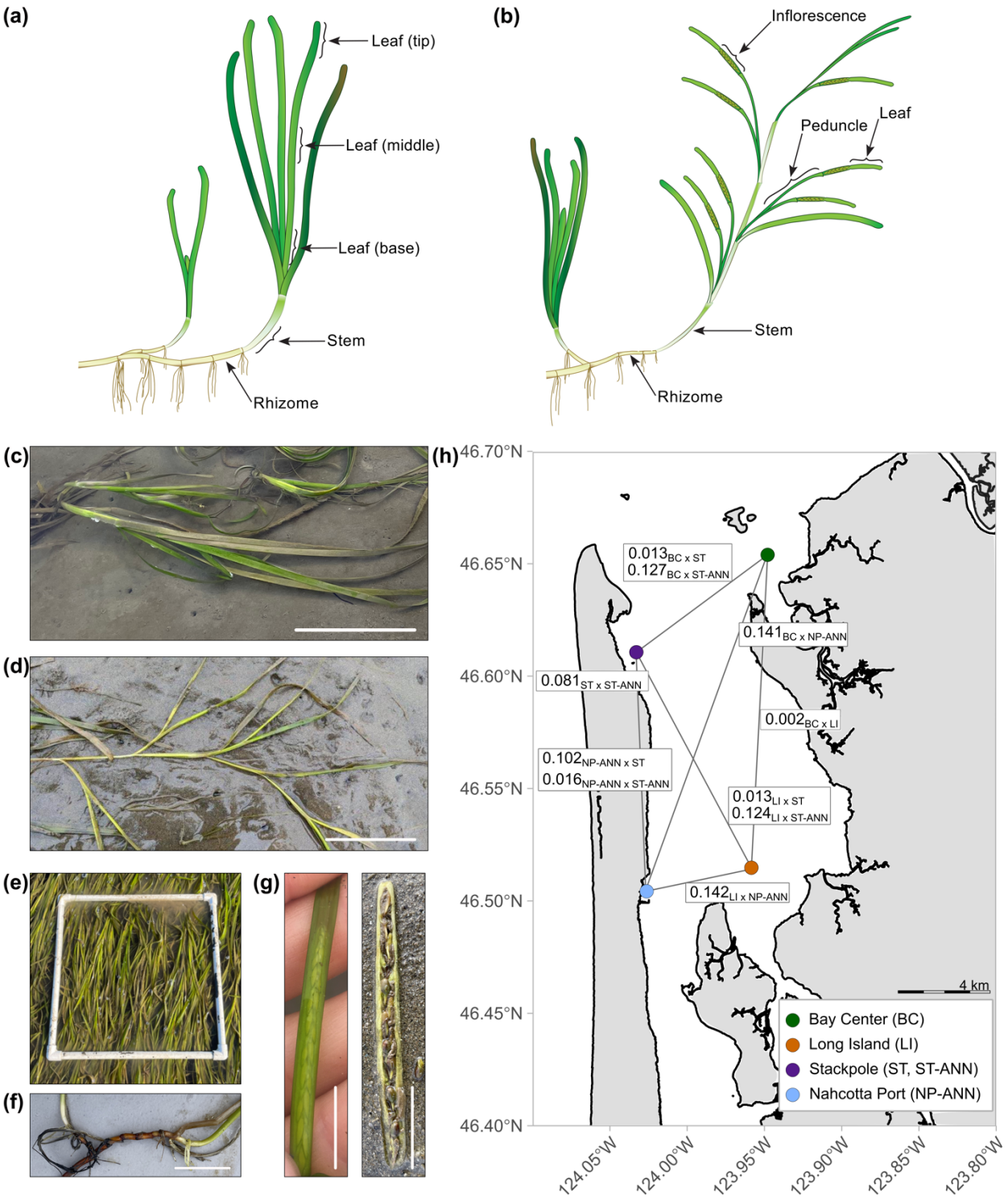

Figure 3: Description of *Zostera marina* (eelgrass) sampling approaches, life stages, and sites used in this study. Tissue isolated from **(a)** vegetative and **(b)** flowering shoots. Eelgrass **(c)** vegetative and **(d)** flowering shoots. Scale bar approximately 10 cm. **(e)** Eelgrass meadows form through **(f)** clonal reproduction via rhizome extension or **(g)** from the formation of inflorescences and seeds within spathes**.** Scale bar approximately 1 cm. **(h)** Geographic location of study sites in Willapa Bay, WA USA: Bay Center (BC), Long Island (LI), Stackpole (ST), Stackpole Annual

964 (ST-ANN) (ST and ST-ANN represented by sample point on map due to proximity), and
965 Nahcotta Port Annual (NP-ANN) (Table S4). Pairwise genetic distance, F_{ST}, estimated through
966 estimated RAD-Seq analysis shown in white boxes (n=48 per population). Subscript of F_{ST}
967 indicates which sites included in the pair-wise comparison. Scale bar approximately 4 km.
968 Photographs of annual plants are in Supplemental Fig. S6.
969

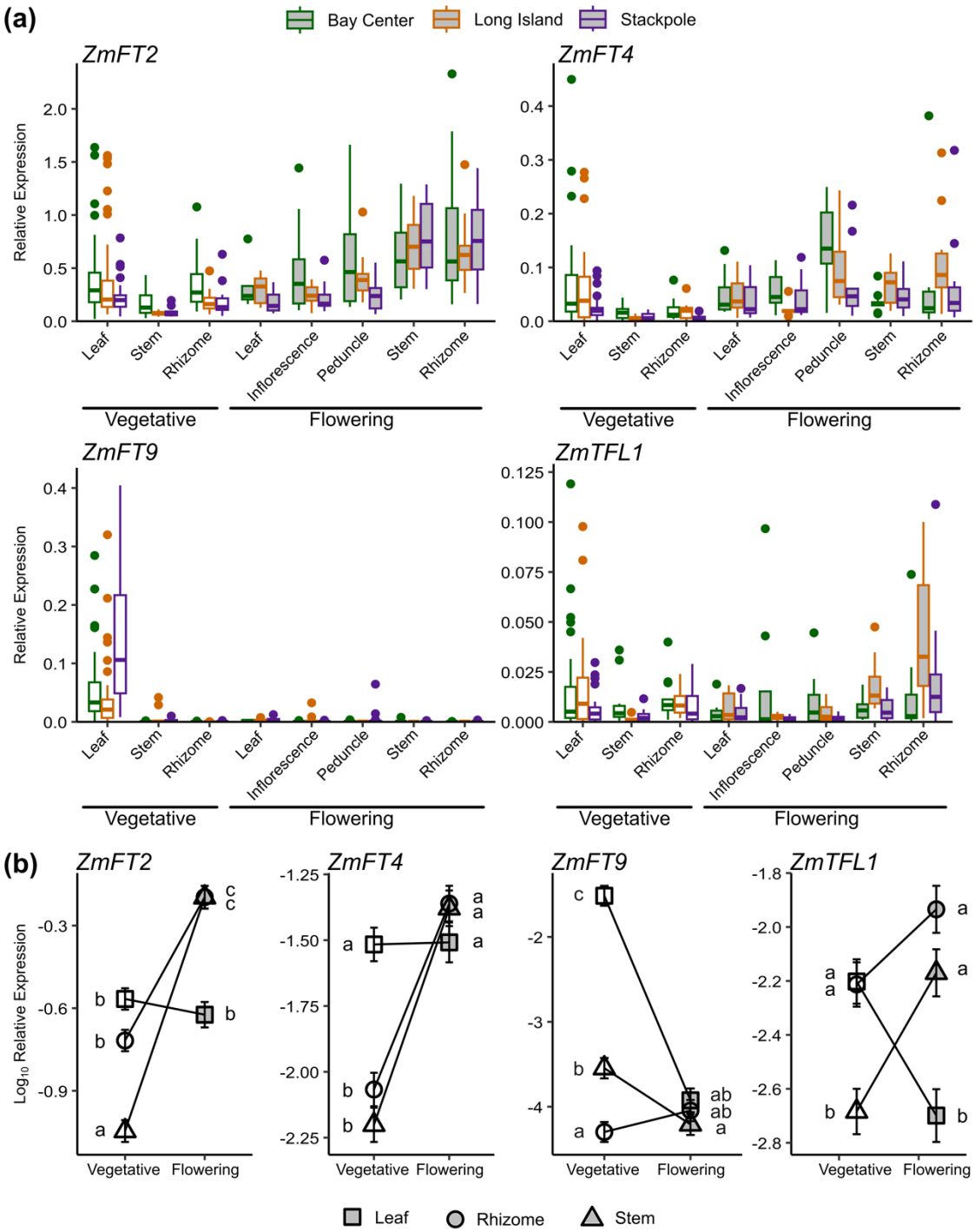

Figure 4: Expression of florigen genes in different *Z. marina* tissues. **(a)** Relative expression levels of *ZmaFT2*, *ZmaFT4*, *ZmaFT9*, and *ZmaTFL1a* across different tissue types in different developmental stages, vegetative (white) and flowering (grey). Expression in tissues was measured in samples (n≥10) from 3 sites shown in Figure 3H. All expression values are relative to 3 reference genes (*CYP2*, *ELF4A*, and *RPL28*). Median is indicated by center line in box, upper and lower quartiles by box boundaries, and highest and lowest values within two interquartile ranges by whiskers. **(b)** Comparing means between tissue types across reveals

978 different trends of expression changes within tissue types across vegetative (white) and flowering
979 (grey) developmental stages. Mean expression was calculated using log_{10} transformed expression
980 values. Error bars are standard errors of means. Different letters indicate statistically significantly
981 different groups determined by one-way ANOVA test with post-hoc Tukey HSD of log_{10}
982 transformed values.
983

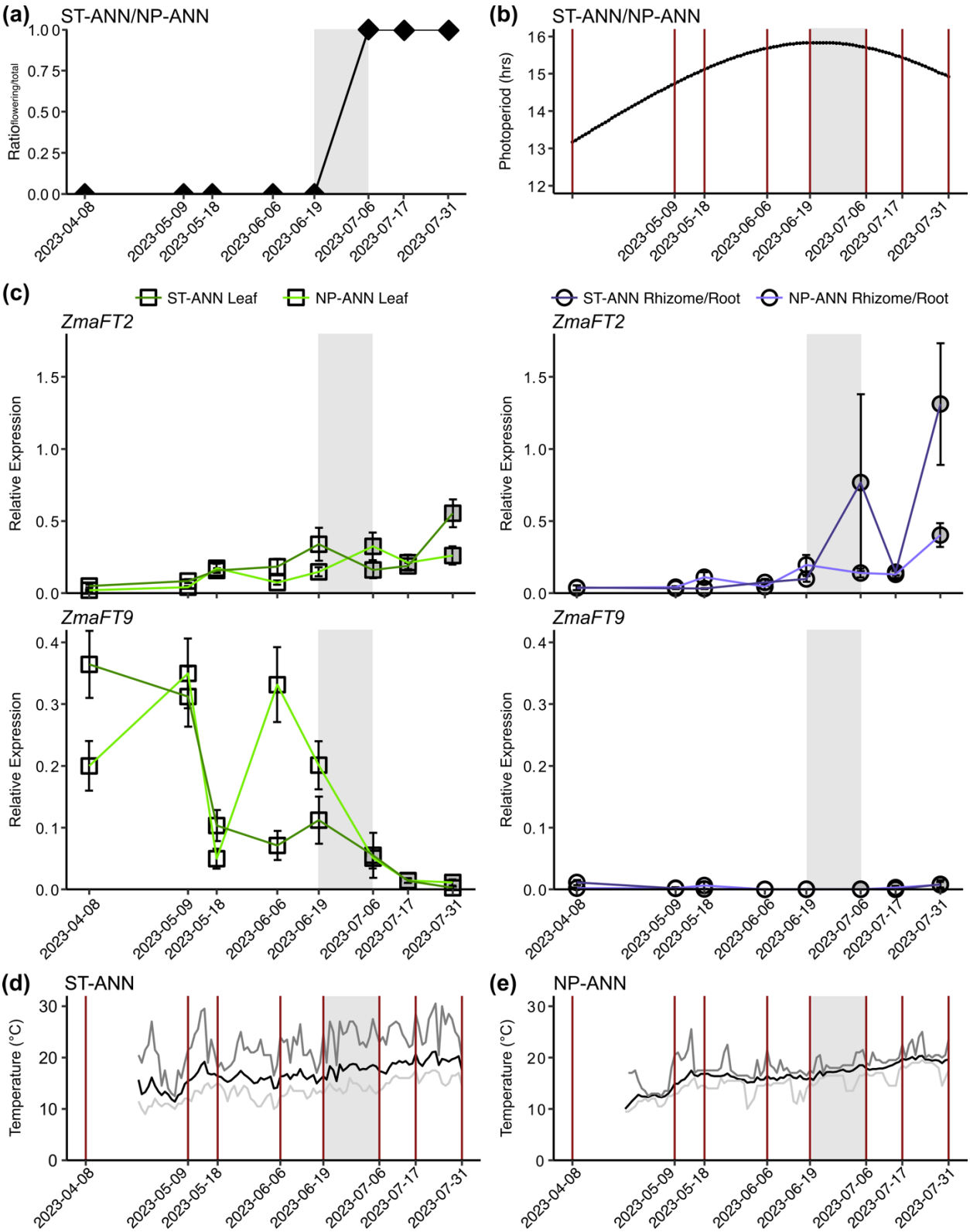

Figure 5: Expression of *ZmaFT2* and *ZmaFT9* genes in leaf and rhizome tissue across the 2023 growing season at ST-ANN and NP-ANN sites (Figure 3H, Table S4). **(a)** Ratio of flowering shoots to total shoots collected at each time point for both ST-ANN populations and NP-ANN

population, n≥10. Grey shaded region in each panel indicates when flowering shoots emerged. **(b)** Photoperiod regime over growing season in Willapa Bay. Data obtained from the US Naval Astronomical Applications Department. Red lines indicate days samples were collected for gene expression analysis. **(c)** Relative expression levels of *ZmaFT2* and *ZmaFT9* across leaf (square) and rhizome and root (circle) throughout the growing season (April-July). Lighter green and purple lines indicate NP-ANN site, while darker green and purple lines indicate ST-ANN site. Time points where shoots are vegetative shown in white and time points where shoots had flowered are filled grey. All expression values are relative to 3 reference genes (*CYP2*, *ELF4A*, and *RPL28*). Plot point represents mean, and error bars are standard error. Statistically significant groupings based on post-hoc Tukey HSD of $\log_{10}$ transformed values are listed in Table S10. **(d, e)** Daily average temperature (black), daily minimum temperature (light grey), and daily maximum temperature (dark grey) at ST-ANN site **(d)** and NP-ANN site **(e)** throughout the growing season. Temperatures were collected at the sediment surface using iButtons (Dallas Semiconductor) every 2 hours. Red lines indicate days samples were collected for gene expression analysis. Temperature from 2023-04-08 to 2023-04-23 was not recorded.